Available online at www.sciencedirect.com
SCIENCE DIRECT®
Applied Energy 83 (2006) 628–648
APPLIED ENERGY
www.elsevier.com/locate/apenergy

Improved condenser design and condenser-fan operation for air-cooled chillers

F.W. Yu *, K.T. Chan

Department of Building Services Engineering, The Hong Kong Polytechnic University, Hung Hom, Kowloon, Hong Kong, China

Received 28 February 2005; revised 6 May 2005; accepted 8 May 2005
Available online 10 August 2005

Abstract

Air-cooled chillers traditionally operate under head pressure control via staging constant-speed condenser fans. This causes a significant drop in their coefficient of performance (COP) at part load or low outdoor temperatures. This paper describes how the COP of these chillers can be improved by a new condenser design, using evaporative pre-coolers and variable-speed fans. A thermodynamic model for an air-cooled screw-chiller was developed, within which the condenser component considers empirical equations showing the effectiveness of an evaporative pre-cooler in lowering the outdoor temperature in the heat-rejection process. The condenser component also contains an algorithm to determine the number and speed of the condenser fans staged at any given set point of condensing temperature. It is found that the chiller's COP can be maximized by adjusting the set point based on any given chiller load and wet-bulb temperature of the outdoor air. A 5.6–113.4% increase in chiller COP can be achieved from the new condenser design and condenser fan operation. This provides important insights into how to develop more energy-efficient air-cooled chillers.

Keywords: Air-cooled chillers; Coefficient of performance; Evaporative pre-cooler; Variable speed condenser fans

* Corresponding author. Tel.: +852 276 64374; fax: +852 276 57198.
E-mail address: befwyu@polyu.edu.hk (F.W. Yu).

0306-2619/$ - see front matter © 2005 Elsevier Ltd. All rights reserved.
doi:10.1016/j.apenergy.2005.05.007

Nomenclature

Symbols

A_{ec}	face area of evaporative pre-cooler (m^2)
AU	overall heat transfer coefficient (kW $°C^{-1}$)
COP	coefficient of performance of chiller
CR	compression ratio
C_{pa}	specific heat-capacity of air (1.02 kJ kg^{-1} $°C^{-1}$)
C_{prg}	specific heat-capacity of vapour refrigerant of evaporator (kJ kg^{-1} $°C^{-1}$)
C_{prl}	specific heat-capacity of liquid refrigerant of condenser (kJ kg^{-1} $°C^{-1}$)
C_{pw}	specific heat-capacity of water (4.19 kJ kg^{-1} $°C^{-1}$)
E	power input (kW)
$E_{cf,ea}$	rated power of one condenser fan (kW)
h_i	specific enthalpy of refrigerant at state "i" (kJ kg^{-1}) (state 1: compressor suction; state 2: compressor discharge; state 3: condenser discharge or expansion-valve inlet; state 4: expansion-valve outlet or evaporator suction)
K_{ex}	characteristic constant of expansion valve
LMTD	log mean temperature-difference (°C)
m_r	refrigerant's mass-flow per compressor (kg s^{-1})
m_w	mass-flow rate of chilled water (kg s^{-1})
N_{cc}	number of staged compressors
N_{cf}	number of staged condenser fans
ni	index of reversible polytropic expansion
P	saturated-refrigerant pressure of the refrigeration circuit (absolute kPa)
PLR	chiller part-load ratio (given by Q_{cl}/Q_{cr})
Q_{cd}	heat rejection (kW)
Q_{cl}	cooling-capacity (kW)
Q_{cr}	nominal cooling-capacity (kW)
q_{rf}	refrigeration effect (kJ kg^{-1})
q_{sw}	water sprinkling density of evaporative pre-cooler (kg m^{-2} s^{-1})
R_{cf}	rotating speed of staged condenser-fans (rps)
R_{cfr}	full speed of condenser fans (15.8 rps)
T	temperature of saturated refrigerant within the refrigeration circuit (°C)
T_{cdae}	temperature of air entering the condenser or outdoor temperature (°C)
T_{cdal}	temperature of air leaving the condenser (°C)
T_{cdsc}	degree of subcooling (°C)
T_{cdsp}	set point condensing temperature (°C)
T_{chwr}	temperature of return chilled-water (°C)
T_{chws}	temperature of supply chilled-water (°C)
T_{evsh}	degree of superheat (°C)
T_i	dry-bulb temperature of air at pre-cooler inlet (°C)
$T_{i,w}$	wet-bulb temperature of air at pre-cooler inlet (°C)

T_o	temperature of air at pre-cooler outlet (°C)
V_a	airflow provided by staged condenser fans ($m^3\ s^{-1}$)
V_{ar}	rated airflow of a variable-speed condenser fan (23.6 $m^3\ s^{-1}$)
V_{vd}	volumetric displacement of each compressor ($m^3\ s^{-1}$)
v_a	face velocity of air through evaporative pre-cooler ($m\ s^{-1}$)
v_r	specific volume of refrigerant at compressor suction ($m^3\ kg^{-1}$)
v'_1	specific volume of saturated vapour refrigerant at evaporator ($m^3\ kg^{-1}$)
w_{in}	isentropic work input to compressor ($kJ\ kg^{-1}$)
ΔE_{cf}	increase in condenser fan power due to evaporative pre-cooler (kW)
ΔP_{ec}	pressure drop across evaporative pre-cooler (kPa)
ΔP_{ex}	pressure drop across expansion valve (kPa)
η_{cc}	combined motor and transmission efficiency
η_{ec}	effectiveness of evaporative pre-cooler
η_{isen}	isentropic efficiency
η_v	volumetric efficiency
ρ_a	air density (1.2 $kg\ m^{-3}$)
ρ_{ex}	density of liquid refrigerant before expansion ($kg\ m^{-3}$)

Subscripts

cc	compressor
cd	condenser
cf	condenser fan
ec	evaporative pre-cooler
ev	evaporator
ex	expansion valve
max	maximum
op	optimum
tot	total

1. Introduction

Air-cooled chillers are widely used to provide cooling energy for commercial and industrial premises but with considerable electricity consumption [1–5]. They traditionally operate under head-pressure control (HPC) via staging constant-speed condenser fans step-by-step. The use of HPC is due to a convention that thermostatic expansion-valves need a high differential between the evaporating and condensing pressures for proper control of the refrigerant flow. In this situation, the condensing temperature will be controlled at above 30 °C at an evaporating temperature of 5 °C. The use of electronic expansion-valves, on the other hand, enables the condensing temperature to drop to as low as 10 °C if there is no problem of compressor lubrication [6,7].

Under HPC, the number of staged condenser-fans is kept minimal. This enables the condensing temperature to hover around a fixed set-point of 45 °C, irrespective

of outdoor temperatures. HPC can bring about fan-power saving, but is ineffective in reducing compressor power when the outdoor temperature drops from a design level of 35 °C. Under HPC, the COP (defined as cooling capacity in kW over chiller power in kW) of air-cooled chillers can drop from 3.1 at full load to 1.2–2.5 at part load for outdoor temperatures ranging from 15 to 35 °C [7].

One pragmatic approach to improving the chiller COP is to lower the condensing temperature to a level that enables the trade-off between compressor power and condenser fan power to be optimized. Using evaporative pre-coolers to enhance the COP of air-cooled chillers is not common, even though the concept is not new. The pre-coolers, when installed in front of air-cooled condensers, can pre-cool outdoor air before entering the condensers while consuming less than 15% of the cooling water required by cooling towers and evaporative condensers [8,9]. For an evaporative pre-cooler, hot air flows across a porous wetted surface with a film of cool water. That air absorbs and evaporates moisture on the surface when leaving the pre-cooler, and then its dry-bulb temperature drops and approaches its wet-bulb temperature. The pre-coolers enable the condensing temperature to drop in response to a reduction in outdoor temperature. However, the pressure drop across the pre-coolers incurs additional fan power.

The potential and benefits of using evaporative pre-coolers hinge on the extent to which the condensing temperature can drop and whether the decrease in compressor power due to this drop can outweigh the additional fan power. Zhang et al. [8] have indicated that the use of evaporative pre-coolers can bring about a 14.7% increase in the COP of air-cooled chillers working in a hot and dry environment. The pre-coolers are expected to have a high effectiveness when cooling outdoor air in a hot and dry climate, but they can function properly even when the climate is hot and humid [9]. Yet there is a lack of research into how to reap the benefits of using evaporative pre-coolers when air-cooled chillers operate in the subtropical climate.

Variable-speed control is increasingly used for chiller compressors to save power when chillers are operating at part load [10–13]. The power saving comes from the improved efficiency of the motors when operating at a lower speed under part-load conditions. However, there is limited evidence to support such control for condenser fans in air-cooled chillers with a nominal cooling capacity of 700–1400 kW. This is probably due to a perception that the use of variable-speed condenser fans has an insignificant effect on the saving of chiller power because the nominal condenser-fan power accounts for less than one-tenth of the nominal compressor power. Furthermore, fan power can be saved by turning off unnecessary constant-speed fans in steps under the existing condenser design. Yet the step-by-step variation in heat-rejection airflow is inappropriate to control the condensing temperature at its set point [6,7]. It is desirable to continuously modulate the heat-rejection airflow via variable-speed fans in order to investigate the trade-off between compressor power and condenser fan power.

Computer simulation is a workable technique to understand the operating characteristics of chillers and to investigate how their COP can be optimized. Many chiller models have been developed using various principles and approaches [14–21]. Among various kinds of chiller models, thermodynamic models are a preferred method to study the steady-state behaviour of a chiller's COP. At present, very few models apply

specifically to air-cooled chillers, and even fewer pertain to air-cooled screw-chillers which become popular in a new installation or retrofit of chiller plants.

To identify the operating variables of chillers with some realism, mechanistic relations between chiller components should be taken into account. The mass balance of refrigerant and energy balances at the evaporator, compressors, expansion valve and condenser have to be satisfied. With regard to the simulation of air-cooled chillers, it is essential to determine the number and speed of condenser fans required to control the condensing temperature at its set point, while meeting the desired airflow for any given heat rejection. Taking all these factors into account, Chan and Yu [6] have developed a thermodynamic model for an air-cooled reciprocating chiller, which considers the real process phenomena, including the capacity control of compressors and variations in the overall heat-transfer coefficients of an evaporator and a condenser at part load. They have also introduced an algorithm to compute the number of staged condenser fans based on a set point condensing-temperature. Chan and Yu's model will form an adequate basis for studying the potential improvements in the chiller's COP when an alternative design for air-cooled condensers is considered.

The aim of this paper is to describe how the COP of air-cooled chillers can be improved by a new condenser design using evaporative pre-coolers and variable speed fans. Using the simulation program TRNSYS [22], a thermodynamic model for an air-cooled screw-chiller was developed and used to study the steady-state behaviour of the chiller's COP under various operating conditions when the design parameters of the condenser change. The model was validated using the performance data in chiller specifications and a wide range of operating data from a field chiller working under HPC. Within the chiller model, the condenser component contains the empirical equations of an evaporative pre-cooler given by Zhang et al. [8] in order to simulate the pre-cooler's effectiveness in lowering the temperature of the outdoor air before entering the condenser. In addition, the condenser component considers a new arrangement for variable-speed condenser fans and an algorithm to compute the number and speed of condenser fans staged to meet any given heat-rejection based on a set-point condensing temperature. The simulation analysis reported here attempts to ascertain the inadequacy of HPC and examine the feasibility of the new condenser design for COP improvements. A new control strategy will be proposed for the operation of variable-speed condenser fans in order to achieve maximum COP under different operating conditions. The interaction between the dryness of the outdoor air and changes in the chiller's COP, due to the use of evaporative pre-coolers, will be discussed.

2. Development of the chiller model

2.1. Configuration and basic assumptions

The configuration of the model chiller is based on a field chiller serving an institutional complex for two years. The operating data of the chiller were monitored year-round by a building-management system. The COP of the chiller at full load

complied with the performance data in the chiller's specifications. The chiller used the refrigerant R134a (tetrafluoroethane) and had a nominal cooling capacity of 1000 kW. The shell-and-tube liquid evaporator worked at a design evaporating-temperature of 3 °C. The temperature of the supply chilled water was set at 7 °C with a temperature rise of 5.5 °C at full load. The flow of chilled water was maintained at 43.0 kg s^{-1} in all operating conditions. The chiller comprised four refrigeration circuits in parallel and each circuit included one electronic expansion valve and one twin-screw compressor. Each compressor provided three steps of capacity control by adjusting the position of the sliding valve. The air-cooled condenser was designed to control the condensing temperature at around 50 °C when the outdoor temperature was 35 °C. To implement HPC, heat rejection was regulated by staging five groups of condenser fans and each group consisted of four constant-speed fans to provide a constant flow of 18.9 m^3 s^{-1}.

With regard to the assumptions of the chiller model, there was no heat exchange between the chiller and its surroundings. This means that heat rejection (Q_{cd}) is the sum of cooling capacity (Q_{cl}) and compressor power (E_{cc}). Changes in the calculated operating variables were independent of time and that means the chiller operated in the steady state. Pressure losses in the refrigerant pipelines were disregarded. The throttling of refrigerant at the expansion valve was assumed to be isenthalpic. The degree of subcooling (T_{cdsc}) and that of superheat (T_{evsh}) were assumed to be 8 and 3 °C, respectively, in all operating conditions, given that their possible variations (T_{cdsc}: 1–6 °C; T_{evsh}: 4–8 °C) caused up to 0.16% of uncertainty of the chiller's COP only [6].

With regard to the uncertainty in the measurement of variables, the temperatures of chilled water were measured by PT100 type temperature-sensors calibrated to an uncertainty of ±0.15 °C at 0 °C and ±0.26 °C at 55 °C. The flow of chilled water was measured by a magnetic flow-meter with an uncertainty of ±2% of actual flow. A power analyser with an uncertainty of ±1% of reading was used to determine the chiller power. The root sum square error of the chiller's COP, due to all the uncertainties of the individual variables, was 7.9–14.6% when the chiller operated at above half load.

The impact of the uncertainty of individual variables on the calculated COP was identified. Table 1 shows how the measurement errors of input variables influenced the calculated results for the chiller's COP when the chiller was operating at full load and at the lowest part-load ratio of 0.083. A unit-bearing sensitivity coefficient (output change over input change) was used to predict the possible uncertainty of the chiller's COP. The percentage uncertainty of the chiller's COP due to each individual input variable is generally lower than the percentage measurement error of that variable. The temperature of the return chilled-water (T_{chwr}) is the most influential variable, responsible for the highest uncertainty of the chiller's COP of 1.16%.

2.2. Methods of simulation

The chiller was modelled by using the simulation program TRNSYS [22]. TRNSYS is based on a modular approach to model chiller components, coded in the form of FORTRAN subroutines. The chiller model was established by creating an input file which linked component subroutines. The subroutine given by Bourdouxhe et al.

Table 1
Uncertainty analysis of operating variables

Input variable	Base case	Perturbations		Input uncertainty	Sensitivity coefficient	Uncertainty of chiller's COP
		min.	max.			
Full load						
T_{chwr} (°C)	12.5	11.5	13.5	0.18 (1.4%)	0.2100	0.0378 (1.156%)
T_{chws} (°C)	7	6	9	0.17 (2.4%)	0.1400	0.0238 (0.728%)
E_{ch} (kW)	305.8	298.8	305.8	3.06 (1%)	0.0114	0.0350 (1.069%)
m_w (kg s^{-1})	43.0	33	50	0.86 (2%)	0.0035	0.0030 (0.093%)
Part-load ratio of 0.083						
T_{chwr} (°C)	7.5	6.5	9.5	0.17 (2.3%)	0.0600	0.0102 (0.312%)
T_{chws} (°C)	7	6	9	0.17 (2.4%)	0.0600	0.0102 (0.312%)
E_{ch} (kW)	61.3	30.4	61.3	0.61 (1%)	0.0447	0.0272 (0.833%)
m_w (kg s^{-1})	43.0	33	50	0.86 (2%)	0.0002	0.0001 (0.005%)

[23] was incorporated into the model to evaluate the thermodynamic properties of the refrigerant R134a. Each operation condition comprised eight inputs: outdoor temperature (T_{cdae}), the wet-bulb temperature of outdoor air ($T_{i,w}$), the chiller part load ratio (PLR), chilled water-flow (m_w), the temperature of supply chilled water (T_{chws}), the degree of subcooling (T_{cdsc}), the degree of superheat (T_{evsh}), and the set-point condensing temperature (T_{cdsp}).

Given that $T_{i,w}$ has no effect on the overall heat-transfer coefficient of an air-cooled condenser alone, it is a compulsory input only when using an evaporative pre-cooler. T_{cdsp} was used to determine the number and speed of the staged condenser fans in order to control the condensing temperature at its set point for any given heat rejection. The outputs are operating variables within the evaporator, compressors, expansion valve and condenser. The chiller's COP is defined as the cooling capacity (Q_{cl}) over chiller power (E_{ch}). It should be noted that E_{ch} is the sum of the compressor power (E_{cc}) and condenser's fan-power (E_{cf}). All outputs were solved by the following sets of algebraic equations through an iterative procedure.

2.2.1. Evaporator

The cooling capacity (Q_{cl}) of an evaporator is expressed by the following equations:

$$Q_{cl} = PLRQ_{cr}, \tag{1}$$

$$= m_w C_{pw}(T_{chwr} - T_{chws}), \tag{2}$$

$$= m_{r,tot} q_{rf}, \tag{3}$$

$$= AU_{ev}\mathrm{LMTD}_{ev}, \tag{4}$$

where

$$q_{rf} = h_1 - h_4, \tag{5}$$

$$AU_{ev} = \frac{1}{c_1 m_w^{-0.8} + c_2 Q_{cl}^{-0.745} + c_3}, \tag{6}$$

$$\mathrm{LMTD}_{ev} = \frac{(T_{chwr} - T_{ev}) - (T_{chws} - T_{ev})}{\ln(\frac{T_{chwr} - T_{ev}}{T_{chws} - T_{ev}})}. \tag{7}$$

The method of log mean temperature-difference (LMTD) was used to model the evaporator and, in turn, to determine the evaporating temperature (T_{ev}). The overall heat-transfer coefficient of the evaporator (AU_{ev}) is described by a simplified mechanistic relation in Eq. (6) [6], where c_1, c_2 and c_3 are characteristic parameters to be evaluated based on the performance data of the chiller. For a constant m_w, AU_{ev} could vary from 27.9 to 151.1 kW °C^{-1}, depending on the load conditions.

2.2.2. Compressors

The actual power input (E_{cc}) of the staged compressors is given by the following equation:

$$E_{cc} = m_{r,tot}\frac{w_{in}}{\eta_{isen}\eta_{cc}}, \tag{8}$$

where

$$m_{r,tot} = \frac{V_{vd}\eta_v}{v_r} N_{cc}, \tag{9}$$

$$w_{in} = P_{ev} v_r \frac{ni}{ni-1}\left(CR^{\frac{ni-1}{ni}} - 1\right), \tag{10}$$

$$CR = \frac{P_{cd}}{P_{ev}} \tag{11}$$

$$\frac{1}{v_r} = \frac{1}{v_{1'}} - (-0.0007 + 0.0002 P_{ev}) T_{evsh}, \tag{12}$$

$$\eta_v = 0.925 - 0.009 CR, \tag{13}$$

$$\eta_{isen} = 0.01(a_1 T_{cd}^2 + a_2 T_{cd} + a_3 T_{ev}^2 + a_4 T_{ev} + a_5 T_{cd}^2 T_{ev} + a_6 T_{cd} T_{ev} + a_7 Q_{cr} + a_8), \tag{14}$$

$$\eta_{cc} = 0.3 + 0.567 PLR + 0.133 PLR^2. \tag{15}$$

The volumetric displacement (V_{vd}) of each constant-speed screw-compressor was 0.12 $m^3\ s^{-1}$ based on the performance data of the chiller at full load. The specific volume of superheated refrigerant at the compressor suction (v_r) was calculated by Eq. (12), which was determined by plotting and fitting the thermodynamic properties of R134a. Volumetric efficiency (η_v) was ascertained by plotting and fitting the compressors' performance data. Eqs. (14) and (15) were used to compute the isentropic efficiency (η_{isen}) and the combined motor and transmission efficiency (η_{cc}) of the screw compressors studied, based on Solati's regression analysis [24]. The constant coefficients a_1 to a_8 of η_{isen} are −0.0316958, 2.90112, −0.0296849, −1.45279, 0.000321176, 0.00683086, 0.0170575 and −16.5018, respectively. With Eqs. (8)–(15), it is possible to assess how compressor power changes in response to different capacity control steps in terms of the PLR and variations in the evaporating temperature (T_{ev}) and condensing temperature (T_{cd}).

The specific enthalpy of the superheated refrigerant at the compressors' discharge (h_2) was solved by using Eq. (16). The specific enthalpy of the superheated refrigerant at the compressor suction (h_1) is given by Eq. (17). The determination of the refrigerant enthalpy at the condenser discharge (h_3) is similar to that of h_1:

$$h_2 = h_1 + \frac{w_{in}}{\eta_{isen}\eta_{cc}}, \tag{16}$$

$$h_1 = h_{1'} + C_{prg} T_{evsh}, \tag{17}$$

$$h_3 = h_{3'} - C_{prl} T_{cdsc}. \tag{18}$$

2.2.3. Expansion valve

The expansion valve was modelled as an isenthalpic process. The total mass-flow rate of the refrigerant ($m_{r,tot}$) is given by Eq. (19), where K_{ex} is a characteristic constant, ρ_{ex} is the density of the liquid refrigerant before expansion and ΔP_{ex} is the pressure difference drop across the expansion valve

$$m_{r,tot} = K_{ex}\sqrt{\rho_{ex}\Delta P_{ex}}. \tag{19}$$

2.2.4. Condenser

Heat rejection (Q_{cd}) involves the energy and mass balance in the condenser and is described by Eqs. (20)–(25). For the overall heat-transfer coefficient of the condenser (AU_{cd}) shown in Eq. (24), the terms with c_4 and c_5 account for the local heat-transfer coefficients of the air side and refrigerant side [6]. The characteristic parameters c_4 to c_6 were determined using the performance data of the chiller. AU_{cd} can be used to describe how a variation in heat-rejection airflow (V_a) influences the control of the condensing temperature (T_{cd}) for any given chiller load. T_{cd} is correlated with the temperature of air entering the condenser (T_{cdae}) and that leaving the condenser (T_{cdal}) by the log mean temperature-difference ($LMTD_{cd}$) defined in Eq. (25)

$$Q_{cd} = Q_{cl} + E_{cc}, \tag{20}$$

$$= m_{r,tot}(h_2 - h_3), \tag{21}$$

$$= V_a \rho_a C_{pa}(T_{cdal} - T_{cdae}), \tag{22}$$

$$= AU_{cd}\mathrm{LMTD}_{cd}, \tag{23}$$

where

$$AU_{cd} = \frac{1}{c_4 V_a^{-0.5} + c_5 m_{r,tot}^{-0.8} + c_6}, \tag{24}$$

$$\mathrm{LMTD}_{cd} = \frac{(T_{cd} - T_{cdae}) - (T_{cd} - T_{cdal})}{\ln\left(\frac{T_{cd} - T_{cdae}}{T_{cd} - T_{cdal}}\right)}. \tag{25}$$

2.2.5. Empirical equations of an evaporative pre-cooler

The following set of empirical equations developed by Zhang et al. [8] was used to evaluate the effectiveness of an evaporative pre-cooler and its pressure drop, and hence to compute the increase in the condenser's fan power. The equations concern a pre-cooler which makes use of corrugated perforated aluminium-foil to provide a wetted surface for pre-cooling outdoor air.

The pre-cooler effectiveness (η_{ec}) is defined by Eq. (26) and can vary from 0.75 to 0.95. As Eq. (27) illustrates, the temperature of air at the pre-cooler outlet (T_o) is correlated with the face velocity of the air through the pre-cooler (v_a), the dry-bulb temperature of the air at the pre-cooler inlet (T_i), the wet-bulb temperature of the air at the cooler inlet ($T_{i,w}$), and water sprinkling density (q_{sw}), i.e. water flow divided by the cross-section area of sprinkling water. The two equations were developed under the following conditions: v_a varied from 2 to 3 m s^{-1}; q_{sw} changed from 0.5 to 1.2 kg m^{-2} s^{-1}; $(T_i - T_{i,w})/T_i$ was between 0.15 and 0.45.

For maximum η_{ec}, q_{sw} was set to be 1.2 kg m^{-2} s^{-1} in all operating conditions. When the equations were incorporated into the condenser component of the chiller model, T_o was equal to the temperature of air entering the condenser (T_{cdae}). Given that the pre-cooler's airflow is the same as the heat-rejection airflow (V_a), v_a varies according to the staging of the condenser fans. Pump power for circulating sprinkling water is negligible compared with the increase in the condenser's fan-power

(ΔE_{cf}) shown in Eq. (28). ΔE_{cf} is due to the pressure drop (ΔP_{ec}) across the pre-cooler, as given by Eq. (29).

$$\eta_{ec} = \frac{T_i - T_o}{T_i - T_{i,w}}, \tag{26}$$

$$T_o = 1.015 T_i^{0.579} T_{i,w}^{0.369} v_a^{0.082} q_{sw}^{-0.03}, \tag{27}$$

$$\Delta E_{cf} = V_a \Delta P_{ec}, \tag{28}$$

$$\Delta P_{ec} = 0.02389 v_a^{2.032} q_{sw}^{0.066}. \tag{29}$$

2.2.6. Algorithm of staging condenser fans

For any given cooling capacity (Q_{cl}), either the heat-rejection airflow (V_a) or condensing temperature (T_{cd}) can be adjusted to meet the required heat-rejection (Q_{cd}) and optimize the trade-off between compressor power and condenser's fan-power. According to HPC, T_{cd} is controlled at slightly below its set point (T_{cdsp}) of 45 °C, as shown in inequality (30). Inequality (31), derived from Inequality (30), describes the minimum required V_a which serves to evaluate the number, and speed if applicable, of the staged condenser-fans.

$$T_{cdal} = \frac{Q_{cd}}{V_a \rho_a C_{pa}} + T_{cdae} < T_{cd} \leqslant T_{cdsp}, \tag{30}$$

$$\frac{Q_{cd}}{\rho_a C_{pa}(T_{cdsp} - T_{cdae})} < V_a. \tag{31}$$

For the existing condenser design with constant-speed fans, V_a is related directly to the number of staged condenser fans (N_{cf}), as shown in Eq. (32). After substituting Eq. (32) into inequality (31), inequality (33) was established to present the correlation between N_{cf} and any given T_{cdsp}. The flow chart in Fig. 1 shows the procedure for evaluating N_{cf} and the power of the staged condenser-fans (E_{cf}).

$$V_a = \frac{V_{a,tot}}{N_{cf,tot}} N_{cf}, \tag{32}$$

$$\frac{N_{cf,tot}}{V_{a,tot} \rho_a C_{pa}} \cdot \frac{Q_{cd}}{(T_{cdsp} - T_{cdae})} < N_{cf}. \tag{33}$$

It is expected that the existing condenser design, with many groups of fans, will pose problems in implementing variable-speed control. There are two major reasons for this: first, it will be difficult to decide whether to reduce the number or speed of the staged condenser fans if V_a drops under part-load conditions. Secondly, it will be difficult to realize the actual power savings from the optimum trade-off between the compressor power and condenser's fan-power if the fans are improperly staged with inadequate rotating speed.

To tackle the difficulties, a new design was proposed for the condenser with which one variable-speed fan was employed for each refrigeration circuit. Given that the chiller studied had four refrigeration circuits, the condenser model contained a total of four variable-speed fans, each of which consumed the rated power of 5.5 kW and

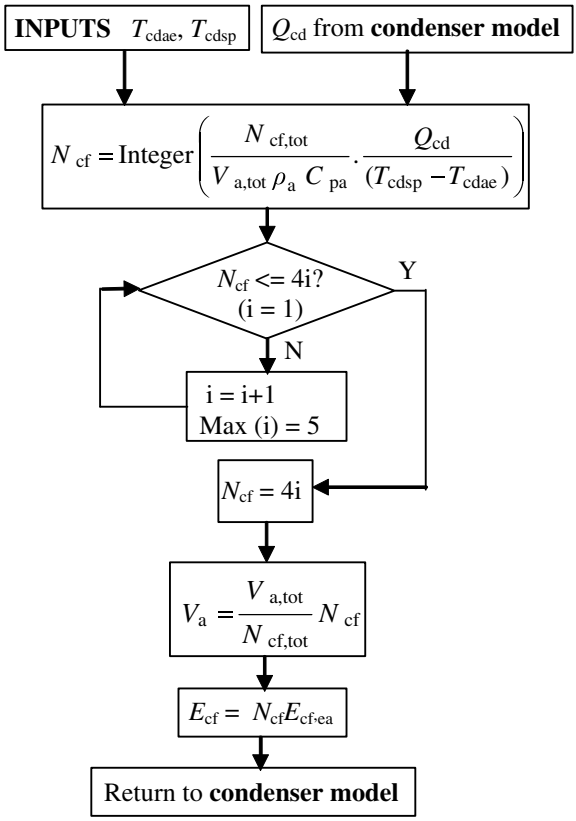

Fig. 1. Procedure for determining the number and power of the staged condenser fans with constant speed.

provided the rated airflow of 23.6 $m^3\ s^{-1}$ at the full speed of 15.8 rps. The condenser fans could operate down to 10% of full speed to give a minimum airflow of 2.36 $m^3\ s^{-1}$. It was assumed that the variable-speed drive consumed 3% of the total power of the staged condenser fans at all speeds.

According to the fan law, the fan speed is directly proportional the fan airflow and the fan power is directly proportional to the fan-speed cubed. Eqs. (34) and (35) were derived from this law and used to calculate the rotating speed of each staged condenser-fan (R_{cf}) and the total power of the staged condenser-fans (E_{cf}). It was assumed that all the staged condenser fans operated at the same speed and the same airflow. One more condenser fan would be staged if the condenser fans staged at full speed were not able to produce the required V_a. When more condenser fans were staged, the heat-transfer area of the condenser could be enhanced and each fan consumed less power at a reduced speed.

The temperature of air entering the condenser (T_{cdae}) depended on V_a since the temperature of the air leaving the pre-cooler (T_o) is a function of V_a along with any combination of the dry-bulb and wet-bulb temperatures (T_i and $T_{i,w}$) of the out-

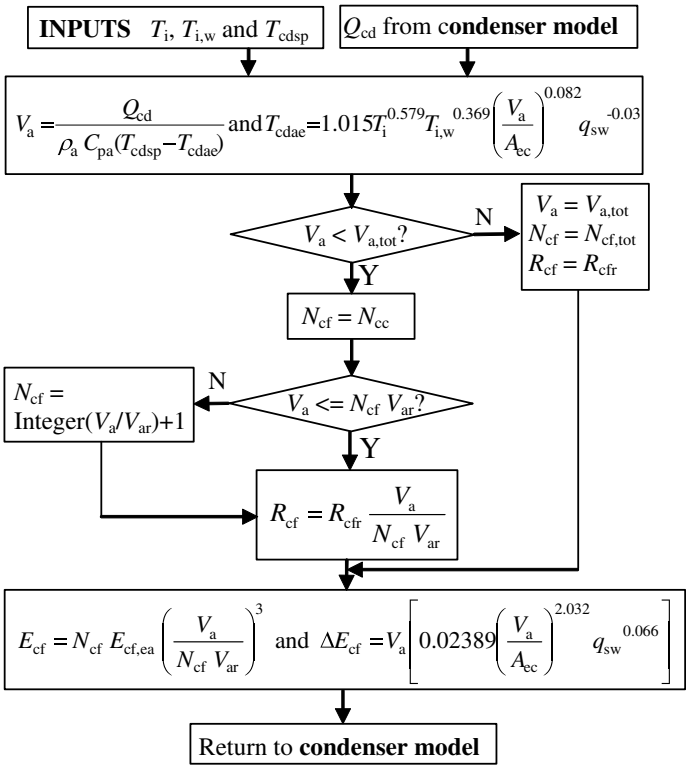

Fig. 2. Procedure for evaluating the number, speed and power of staged condenser-fans.

door air. Regarding this, Newton's method was applied to solve V_a and T_{cdae}. The variables and additional fan-power (ΔE_{cf}) associated with the evaporative pre-cooler were then computed with the calculated V_a and T_{cdae}. In the calculation of chiller power (E_{ch}), ΔE_{cf} was considered along with E_{cc} and E_{cf}. Fig. 2 shows the procedure for calculating N_{cf}, R_{cf}, E_{cf} and ΔE_{cf}

$$R_{cf} = R_{cfr}\frac{V_a}{N_{cf} V_{ar}}, \tag{34}$$

$$E_{cf} = N_{cf} E_{cf,ea}\left(\frac{V_a}{N_{cf} V_{ar}}\right)^3. \tag{35}$$

3. Evaluation of operating variables

The flow charts in Fig. 3 show the procedure for evaluating the operating variables of the chiller components. The evaporator component was computed from the variables (T_{chwr}, AU_{ev} and $LMTD_{ev}$) based on the inputs: the PLR, chilled-water flow (m_w), temperature of supply chilled-water (T_{chws}) and degree of superheat

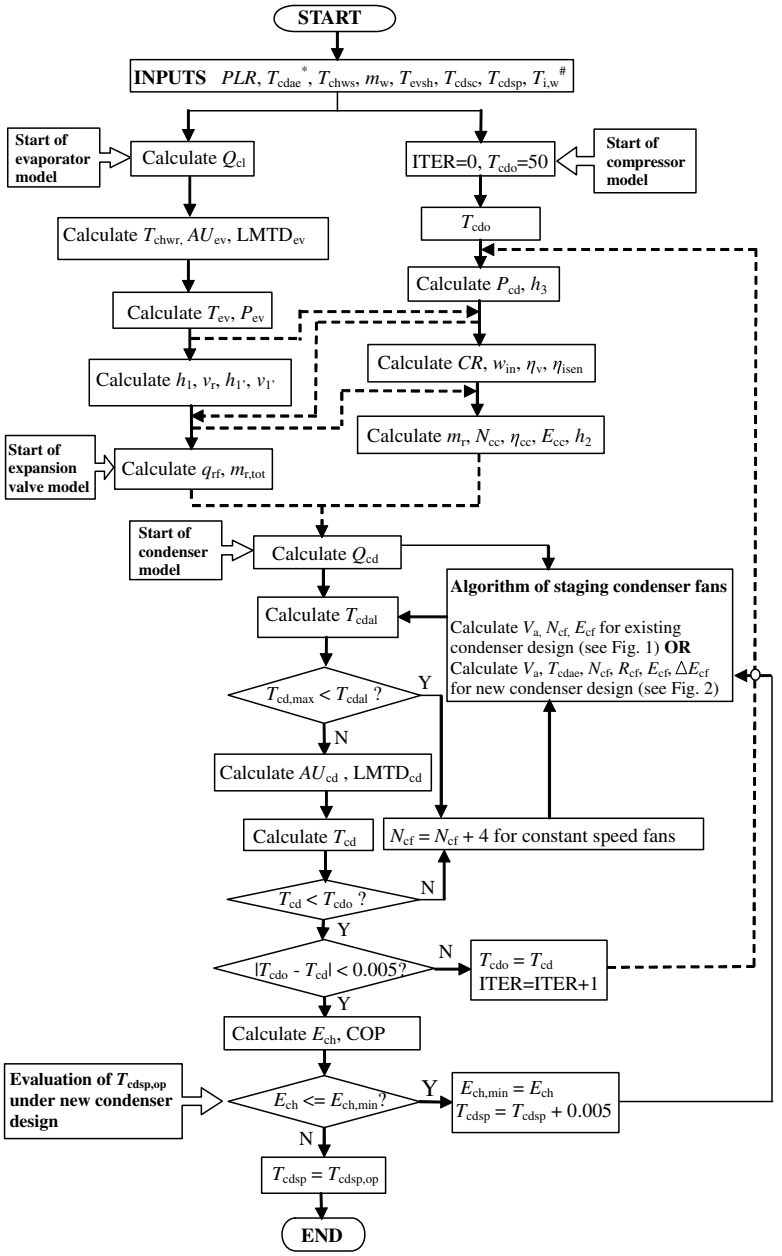

*. T_{cdae} is a direct input variable under existing condenser design or a calculated variable based on T_i and $T_{i,w}$ under new condenser design.
#. The wet-bulb temperature of outdoor air is considered for the new condenser design only.
The dotted arrows represent the links between different chiller component models.

Fig. 3. Procedure for determining the operating variables of the model chiller.

(T_{evsh}). Then the outputs, evaporating temperature (T_{ev}) and pressure (P_{ev}), and refrigerant properties at compressor suction (h_1 and v_r) were calculated. Given that the condensing temperature (T_{cd}) linked the compressor and condenser components, the operating variables of the two components had to be solved altogether at a specific accuracy through an iterative procedure. This started with an initial condensing temperature (T_{cdo}) of 52 °C in the compressor component (the case: ITER = 0). Using Eqs. (8)–(19), the variables within the compressor and expansion valve components were determined directly. The inputs to the condenser component consisted of outdoor temperature (T_{cdae}), compressor power (E_{cc}) and outputs of the evaporator and expansion components (Q_{cl} and $m_{r,tot}$). When the evaporative pre-cooler was used, the wet-bulb temperature of the outdoor air ($T_{i,w}$) constituted another input to the condenser component. Heat rejection (Q_{cd}) and all other variables could then be solved by the equations of the condenser component.

When the simulation was carried out on the chiller operating under HPC, the number of staged condenser-fans (N_{cf}) and the corresponding airflow (V_a) were computed according to a fixed T_{cdsp} of 45 °C. There were three logical arguments in the flow chart of the condenser model to ensure the reliability of all the calculated variables. In the first argument, if the temperature of air leaving the condenser (T_{cdal}) solved by Eq. (22) exceeded the maximum condensing temperature ($T_{cd,max}$) of 52 °C, one more group of condenser fans would be added to raise the airflow and to reduce the condensing temperature subsequently calculated to below 52 °C. In the second argument, if the condensing temperature calculated in the condenser component was greater than that calculated previously in the compressor component, one more fan group would be staged to bring it to its set point. In the third argument, if the difference between the condensing temperature and its previous value lay within ±0.005 °C, all variables would be solved in equilibrium; otherwise the next value of the condensing temperature would substitute for its previous one to perform the next iteration until the required accuracy was met.

When the new condenser design, with an evaporative pre-cooler and variable-speed fans were present, one more logical argument was included in the condenser component to determine the optimum T_{cdsp} ($T_{cdsp,op}$) for maximum chiller COP. This argument checked the change in chiller power when T_{cdsp} increased in steps of 0.005 °C from its boundaries of 20–45 °C. The lower boundary is intended for ensuring proper oil-viscosity for compressor lubrication [6] and the upper boundary is based on HPC. For each operating condition, the minimum chiller power along with the optimum T_{cdsp} were able to be identified when the change in chiller power varied from a negative value to a positive value.

4. Results and discussion

4.1. Validation of the chiller model

The measured data used for validating the chiller model came from a field chiller operating under HPC. These data belonged to the COP of the field chiller in the

steady state at various outdoor temperatures (T_{cdae}: 15–34 °C) and part-load ratios (PLR: 0.25–1). Each set of inputs of the chiller model contained a certain combination of T_{cdae} and PLR, and around 50 discrete combinations were selected for the validation. For HPC, the set-point condensing temperature (T_{cdsp}) was fixed at 45 °C, irrespective of the chiller load or outdoor temperature. For all combinations of T_{cdae} and PLR, the inputs (m_w, T_{chws}, T_{cdsc} and T_{evsh}) were regarded as constants as specified in Section 2.1. Fig. 4 illustrates that the modelled results of the chiller's COP agreed well with the corresponding measured data. For 86% of data points, the uncertainty of the chiller's COP was less than 10%, and for half of these the uncertainty was even within ±5%. With this good agreement, it is justifiable to use the chiller model to investigate how the new condenser design helps improve the chiller's COP in various operating conditions.

4.2. Optimum set-point condensing temperature with the new condenser design

When the evaporative pre-cooler and variable-speed fans were used, the dry-bulb and wet-bulb temperatures (T_i and $T_{i,w}$) of the outdoor air constituted as inputs to the chiller model. Table 2 summarizes the T_i and $T_{i,w}$ used in the simulation analysis. Each weather condition refers to a combination of T_i and $T_{i,w}$ which complied with the pre-cooler's requirement that $(T_i - T_{i,w})/T_i$ should be between 0.15 and 0.45. The chiller operated at each PLR under these weather conditions.

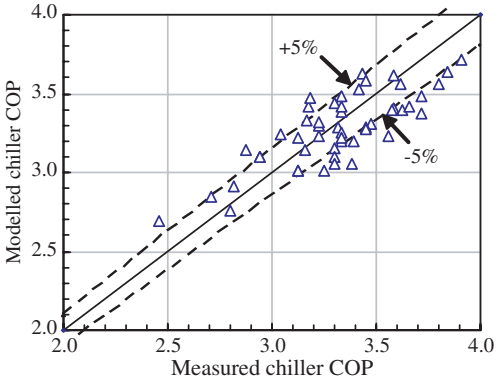

Fig. 4. Comparison between the modelled and measured data of the chiller coefficient of performance (COP).

Table 2
Combinations of the dry-bulb and wet-bulb temperatures (T_i and $T_{i,w}$) of outdoor air for inputs into the chiller model

Dry-bulb temperature T_i (°C)	Wet-bulb temperatures $T_{i,w}$ (°C)				Relative humidity range (%)
15	8.25	9.75	11.25	12.75	38–78
20	11	13	15	17	31–74
25	13.75	16.25	18.75	21.25	25–72
30	16.5	19.5	22.5	25.5	23–70

For each operating condition, it is possible to identify the optimum set-point condensing temperature ($T_{cdsp,op}$) at somewhere between 20 and 45 °C. Fig. 5 shows how $T_{cdsp,op}$ varied under different operating conditions. $T_{cdsp,op}$ generally increased with $T_{i,w}$ and chiller part-load ratios. When the outdoor temperature was 20 °C or below, $T_{cdsp,op}$ tended to oscillate at lower chiller-loads. At these chiller loads, a slight variation in T_{cdsp} made no appreciable change on the heat-rejection airflow, but could alter the number of staged condenser fans, which in turn resulted in large fluctuations in their rotating speed and power. It is confirmed that maintaining a fixed T_{cdsp} of 45 °C under HPC cannot bring about an optimum trade-off between compressor power and condenser fan-power. With a high and fixed T_{cdsp}, the potential decrease in the compressor power is ignored, though the condenser fan power tends to be minimal.

With the evaporative pre-cooler, T_{cdsp} depended on the wet-bulb temperature of the outdoor air ($T_{i,w}$) rather than the dry-bulb one (T_i). This is because the extent to which $T_{i,w}$ differs from T_i influences the pre-cooler effectiveness in reducing the temperature of air entering the condenser (T_{cdae}). Given this situation, $T_{cdsp,op}$ can be set at below T_i in many operating conditions. The lower boundary of T_{cdsp} can drop to as low as ($T_{i,w}$ + 2.3) °C, while that of T_{cdsp} should be at least (T_i + 5) °C under the existing condenser design [6,7]. $T_{cdsp,op}$ can be achieved by adjusting T_{cdsp} based on

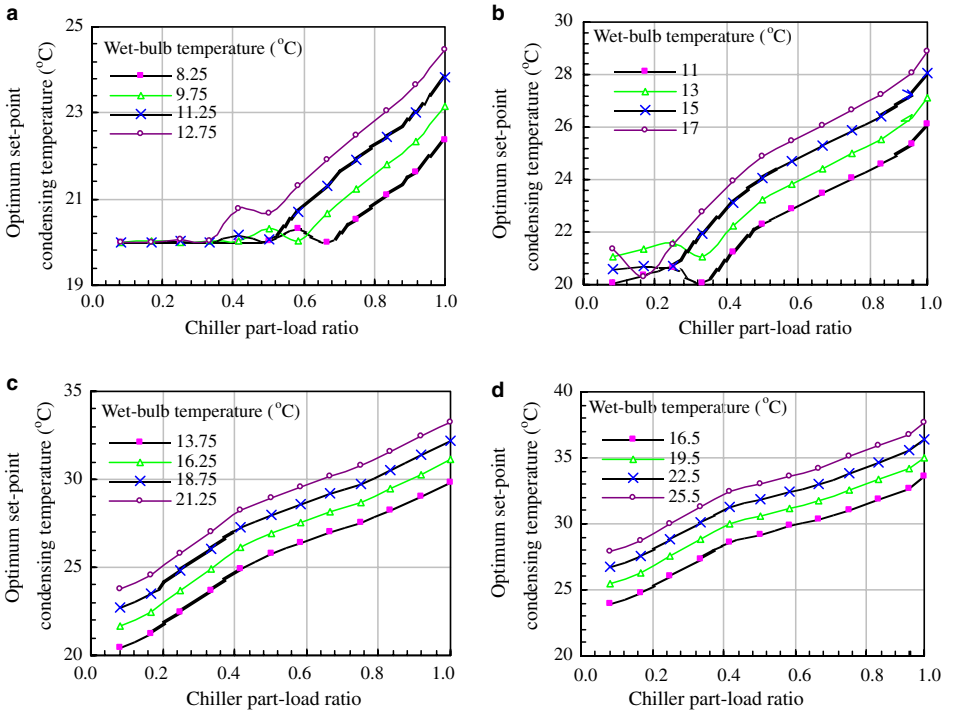

Fig. 5. Optimum set points of condensing temperature at different combinations of dry-bulb and wet-bulb temperatures of outdoor air: (a) outdoor temperature = 15 °C; (b) outdoor temperature = 20 °C; (c) outdoor temperature = 25 °C; (d) outdoor temperature = 30 °C.

any given *PLR* and $T_{i,w}$. It is envisaged that such adjustment in the set-point condensing temperature is applicable to maximizing the COP of large chiller systems with evaporative condensers. This is because the specification of the effectiveness of evaporative condensers is based on the wet-bulb temperature of the outdoor air.

Some researchers [25,26] opined that $T_{cdsp,op}$ should be adjusted in response to the wet-bulb temperature of the outdoor air alone – which is independent of the chiller's load – in order to enhance the performance of chillers with evaporative condensers. This seems to contradict the present finding that $T_{cdsp,op}$ should exceed $T_{i,w}$ by 2.3–18.0 °C, depending on the chiller part-load ratios of 0.083–1. As Chan and Yu [6] state, reducing the condensing temperature to its lower boundary is a possible means to achieve an optimum trade-off between compressor power and condenser fan-power when constant-speed condenser fans are considered. For the new condenser design, with variable-speed fans, their power consumption drops considerably at lower speeds. This can influence the trade-off between compressor power and condenser fan-power under different chiller-load conditions. $T_{cdsp,op}$ needs to increase with the chiller load when the increase in compressor power can be more than offset by the power saving of condenser fans at lower speed. The increasing $T_{cdsp,op}$ signals how the speed of the staged condenser fans can drop to meet the required heat rejection while maximum chiller COP is achieved. The staging and speed of the condenser fans will change from time-to-time in response to the varying set-point condensing temperature.

All these findings suggest that a more sophisticated control algorithm for the adjustment in T_{cdsp} should be included in chiller's microprocessors in order to achieve the improved chiller COP with the new condenser design and condenser fan operation.

4.3. Improved chiller COP under the new condenser design

It is worth investigating the improved COP with the optimum T_{cdsp} under the new condenser design and condenser-fan operation. Fig. 6 gives a comparison between the COP under the traditional condenser design with HPC and that under the new condenser design with $T_{cdsp,op}$. Under HPC with constant-speed condenser fans, the heat-rejection airflow varied in a discontinuous manner, causing a fluctuation in the chiller's COP across the entire range of part-load ratios, especially when the outdoor temperature was low. The troughs in the chiller's COP resulted from a situation where the condensing temperature hovered well above its set point because the airflow supplied deviated from the minimum airflow required.

Under the new condenser design, the continuous modulation of the heat-rejection airflow enabled the condensing temperature to be controlled close to its set point. The chiller's COP could rise almost linearly with *PLR*. With the use of the pre-cooler, the chiller's COP could be improved further when the outdoor air was dry with a large difference between the dry-bulb and wet-bulb temperatures. Considering that the control of the condensing temperature is based on the wet-bulb temperature, rather than the dry-bulb temperature, of outdoor air, the heat-rejection capacity of the condenser can be enhanced throughout the entire range of chiller loads. Under

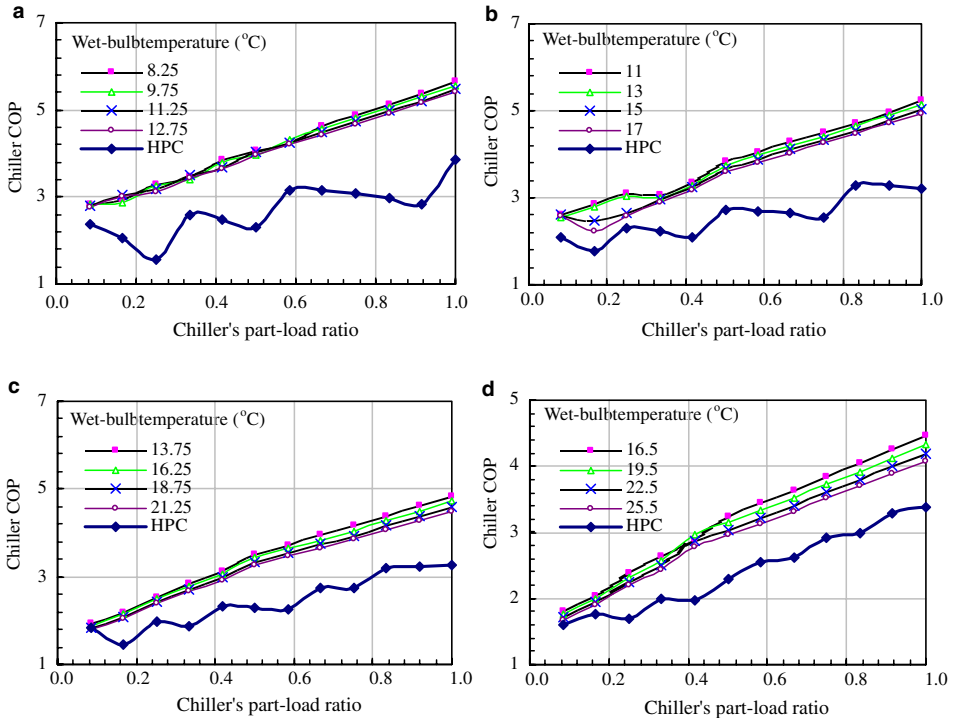

Fig. 6. Improved chiller's COP in various operating conditions at different combinations of dry-bulb and wet-bulb temperatures of outdoor air: (a) outdoor temperature = 15 °C; (b) outdoor temperature = 20 °C; (c) outdoor temperature = 25 °C; (d) outdoor temperature = 30 °C.

these circumstances, a considerable improvement in the chiller's COP at full load could occur. Due to the improved condenser design and condenser-fan operation, there is a 5.6–113.4% increase in chiller COP, depending on the operating conditions.

Because of the lowering of the condensing temperature with the new condenser design, the refrigeration effect (q_{rf}) and hence cooling capacity increased by 3.8–28.2%. The increased cooling capacity could enable the staged compressors to operate at higher loads for a longer time, which, in turn, could alleviate their wear and tear problem due to frequent on–off switching. Chillers with the increased cooling capacity could carry higher loads with higher COPs more frequently when the chiller sequencing is properly implemented in a multiple-chiller plant. This could result in a further reduction in the electricity consumption of chillers.

5. Conclusions

This paper presents the potential improvements in the COP of air-cooled screw-chillers, when their condensers are designed with evaporative pre-coolers and vari-

able-speed fans. A thermodynamic model for an air-cooled screw chiller was developed and validated using chiller specifications and a wide range of operating data in the steady state. Within the model, the condenser component considers empirical equations which model the extent to which the temperature of the outdoor air entering the condenser can drop when an evaporative pre-cooler is used. The condenser component also contains an algorithm to determine the number and speed of condenser fans staged at any given set-point condensing temperature. Using the validated model, the optimization of the set point condensing temperature for maximum chiller COP was studied.

It is found that the optimum set-point condensing temperature is a function of chiller load and the wet-bulb temperature of the outdoor air. This shows the possibility to use evaporative pre-coolers to further lower the condensing temperature in order to save compressor power. This also highlights the dynamic interaction between the compressor power and the condenser's fan-power under various chiller load conditions when variable speed fans are considered. Using the new condenser design and condenser fan operation, there is a 5.6–113.4% increase in the chiller's COP, depending on the chiller loads and weather conditions. Along with the improved chiller COP, cooling capacity can be enhanced by 3.8–28.2%, which enables the chillers to operate at higher loads.

The chiller model will be useful in estimating the likely electricity savings of air-cooled chillers with the improved condenser design when these chillers handle a cooling-load profile. Such estimation could help chiller manufacturers decide if a new condenser design is a feasible investment for the development of more energy-efficient air-cooled chillers. It could also enable chiller purchasers to assess whether the reduced electricity costs are worth the capital costs of the chillers with the improved COP. Based on the potential electricity-savings, energy planners could formulate relevant policies to foster the use of more energy-efficient air-cooled chillers.

Acknowledgement

The work described in this paper was supported by a grant from the Research Grants Council of the Hong Kong SAR, China (Project No. PolyU 5113/04E).

References

[1] Chan KT, Yu FW. Applying condensing-temperature control in air-cooled reciprocating water chillers for energy efficiency. Appl Energy 2002;72:565–81.
[2] Chan KT, Yu FW. Part-load efficiency of air-cooled multiple-chiller plant. Building Services Eng Res Technol 2002;23(1):31–41.
[3] Lam JC. Energy analysis of commercial buildings in subtropical climates. Building Environ 2000;35:19–26.
[4] Yik FWH, Burnett J, Prescott I. Predicting air-conditioning energy consumption of a group of buildings using different heat-rejection methods. Energy Buildings 2001;33:151–66.

[5] Yu FW, Chan KT. Electricity end-use characteristics of air-cooled chillers in hotels in Hong Kong. Building Environ 2005;40(1):143–51.
[6] Chan KT, Yu FW. Optimum set-point condensing temperature for air-cooled chillers. Int J HVAC&R Res 2004;10(2):113–27.
[7] Yu FW, Chan KT. Experimental determination of the energy efficiency of an air-cooled chiller under part-load conditions. Energy 2005;30(10):1747–58.
[8] Zhang H, You SJ, Yang HX, Niu JL. Enhanced performance of air-cooled chillers using evaporative cooling. Building Services Eng Res Technol 2000;21(4):213–7.
[9] Bom GJ, Foster R, Dijkstra E, Tummers M. Evaporative air-conditioning: applications for environmentally-friendly cooling (World Bank technical paper no. 421. energy series). Washington, DC: World Bank; 1999.
[10] Aprea C, Mastrullo R, Renno C, Vanoli GP. An evaluation of R22 substitutes performances regulating continuously the compressor refrigeration capacity. Appl Thermal Eng 2004;24(1):127–39.
[11] Hartman T. All-variable speed centrifugal chiller plants. ASHRAE J 2001;43(9):43–53.
[12] Koury RNN, Machado L, Ismail KAR. Numerical simulation of a variable-speed refrigeration system. Int J Refrig 2001;24:192–200.
[13] Tassou SA, Quereshi TQ. Comparative performance evaluation of positive-displacement compressors in variable-speed refrigeration applications. Int J Refrig 1998;21(1):29–41.
[14] Gordon JM, Ng KC, Chua HT. Optimizing chiller operation based on finite-time thermodynamics: universal modeling and experimental confirmation. Int J Refrig 1997;20(3):191–200.
[15] Bourdouxhe JP, Grodent M, Lebrun JJ, Saavedra C, Silva KL. A toolkit for primary HVAC system energy calculation – part 2: reciprocating chiller models. ASHRAE Trans 1994;100(2):774–86.
[16] Browne MW, Bansal PK. Transient simulation of vapour-compression packaged liquid chillers. Int J Refrig 2002;25:597–610.
[17] Jia Y, Reddy TA. Characteristic physical parameter approach to modeling chillers suitable for fault detection, diagnosis, and evaluation. J Solar Energy Eng 2003;125(August):258–65.
[18] Khan JR, Zubair SM. Design and performance evaluation of reciprocating refrigeration systems. Int J Refrig 1999;22:235–43.
[19] Wang SW. Dynamic simulation of a central chilling system and evaluation of EMCS on-line control strategies. Building Environ 1998;33(1):1–20.
[20] Solati B, Zmeureanu R, Haghighat F. Correlation based models for the simulation of energy performance of screw chillers. Energy Conversion Manage 2003;44(12):1903–20.
[21] Ding G, Fu L. Performance analysis and improvement of air-to-water chiller for application in wide ambient temperature range. Appl Thermal Eng 2004;25(1):135–45.
[22] Solar Energy Laboratory. TRNSYS: A transient system simulation program (Reference manual). Madison, WI: University of Wisconsin-Madison Press; 2000.
[23] Bourdouxhe JP, Grodent M, Lebrun JJ. A toolkit for primary HVAC system energy calculation [Computer program]. Atlanta, GA: American Society of Heating, Refrigerating and Air-Conditioning Engineers; 1995.
[24] Solati B. Computer modeling of the energy performance of screw chillers (M.Sc. thesis). Department of Building, Civil and Environmental Engineering. Montreal, Quebec: Concordia University Press; 2002.
[25] Manske KA, Reindl DT, Klein SA. Evaporative condenser control in industrial refrigeration systems. Int J Refrig 2001;24:676–91.
[26] Briley GC. Energy conservation in industrial refrigeration systems. ASHRAE J 2003;45(6):46–7.